Supplementary Materials: Powering a Sustainable and Circular Economy—An Engineering Approach to Estimate Renewable Energy Potentials within Earth System Boundaries

Harald Desing *, Rolf Widmer, Didier Beloin-Saint-Pierre, Roland Hischier and Patrick Wäger

1. Energy Fluxes and Classification of RE Resources

The Earth system is powered by three energy potentials emanating from inaccessible resources: solar irradiance fed from solar fusion processes, geothermal heat flux fed from residual heat, fission, and crystallization processes, as well as tides fed from rotational inertia of the gravitationally coupled earth–moon–sun system. In this text, these incoming energy fluxes (synonymous to flows) are considered constant over long time spans and inexhaustible. In the Earth system, they are balanced exclusively by terrestrial albedo and excitance, that is, with two radiant fluxes of non-overlapping spectra: reflected short wave (i.e., solar 5760 K) and emitted long wave (i.e., terrestrial 255 K).

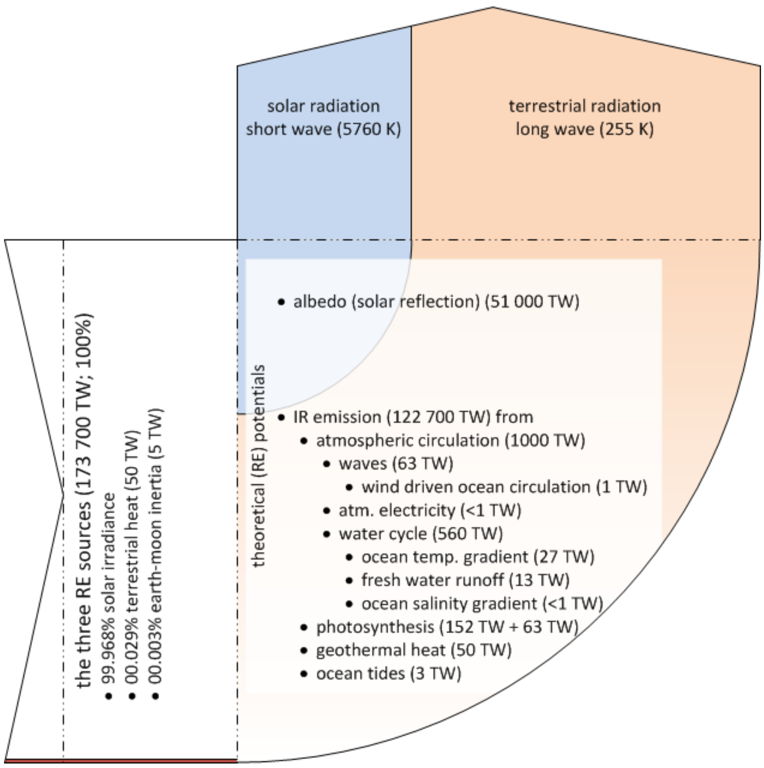

Figure S1. Schematic overview of the energy fluxes in the undisturbed Earth system (data from [1] and NASA https://earthobservatory.nasa.gov/features/EnergyBalance.

In this context, we adhere to the SI terms and units of radiometry (wikipedia) and use joule for energy in general, watt for energy fluxes ($1\,\mathrm{W} = 1\,\mathrm{J\,s^{-1}}$), and watt divided by square meter for flux densities ($1\,\mathrm{W\,m^{-2}} = 1\,\mathrm{J\,s^{-1}\,m^{-2}}$). In this text, e.g., an annual energy demand in tonnes of oil equivalent (toe) is referred to as an energy flux expressed in watts; the quantity *toe* is converted to SI with $toe/\mathrm{GJ} = 41.868$ and with $\mathrm{a\,s^{-1}} = 3.156 \times 10^7$ (seconds in one year) to a flux $41.868\,\mathrm{GJ\,a^{-1}} = 41.868\,\mathrm{GW\,s\,a^{-1}} = 41.868/(3.156 \times 10^7)\,\mathrm{GW} = 1.33\,\mathrm{kW}$. Or, e.g., the annual insolation, the solar irradiance cumulated over one year, is a radiant exposure and is expressed in joules per square meter $1\,\mathrm{J\,m^{-2}} = 1\,\mathrm{W\,s\,m^{-2}} = 1/(3.156 \times 10^7)\,\mathrm{W\,a\,m^{-2}}$.

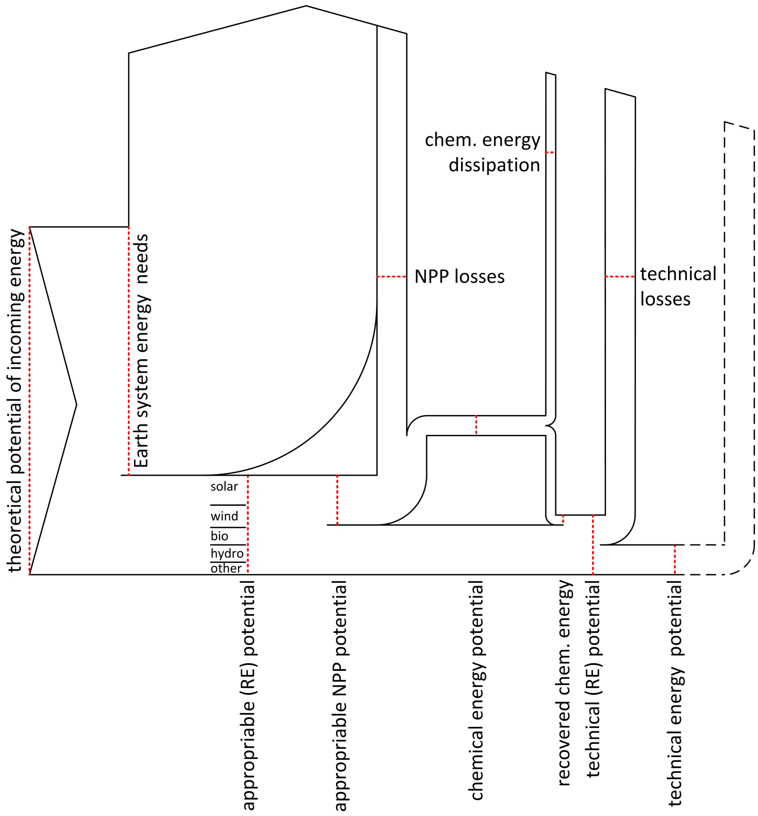

Figure S2. Schematic overview of the energy fluxes in the Earth system with the human appropriation of chemical and technical energy.

Following the cascading conversion chain of an incoming energy flux, the occurring RE resources are classified according to the pathway through the Earth system. Other possibilities are to classify the energy resources according to conversion technologies (e.g., heat engine) or energy form (e.g., kinetic energy).

All RE potentials, except terrestrial heat and tides, originate from solar irradiance. An almost constant energy flux of 1.7×10^{17} W reaches Earth at the top of the atmosphere (TOA), out of which approximately 30 % is reflected without much interaction with the Earth system. Approximately 21 % is absorbed in the atmosphere. Approximately 2/3 of the solar irradiance reaches the surface on ocean and the rest on land. The spatially and temporally varying irradiation is absorbed by and unevenly heats the different surfaces resulting in (a) long wave IR emission and (b) important temperature gradients leading to convective and conductive heat transfer in the atmosphere. Due to the greenhouse effect by greenhouse gases (GHG), vast amounts of long wave IR radiation (almost twice the solar irradiance) are exchanged between the troposphere and the surface. Air currents which tend to equalise the atmospheric temperature gradients [1–6] are an available energy potential (mainly horizontal winds) and can be appropriated and converted to technical energy via *wind power* technologies.

Plants convert solar irradiance to chemical energy in biomass (net primary production, NPP). This primary biomass is the sole energy input to the trophic chain, supporting all other life forms. The available energy potential of surface irradiance as well as NPP can be appropriated and converted into technical energy.

Energy absorbed in the surface layer of water bodies leads to a vertical temperature gradients which *ocean thermal energy conversion* devices can convert to technical energy. Dried continental air moving over the warmed water surface enables continuous evaporation, which desalinates sea water and feeds the global water cycle [7]. Water vapor is transported by winds and precipitates partly over land. The water runoff from land driven by the potential energy of the elevated water carries sediments and nutrients back to the ocean. The available part of this potential can be appropriated and converted into technical energy via *hydro power* plants.

When the freshwater runoff mixes with salty ocean waters, the chemical potential between fresh and salt water is dissipated as low temperature heat. The available part of this potential can be appropriated and converted to technical energy via *forward osmosis* devices, which utilize osmotic pressure differences.

The shearing forces on water surface exerted by wind cause the formation of waves and currents. The available energy potential of water waves can be appropriated/harvested via *wave power* plants.

Additional to solar energy, a comparatively small terrestrial heat flux from residual heat, crystallization, and nuclear fission in Earth's core and mantel of about 3.1×10^{13} W [4] reaches via conduction and convection as low temperature heat Earth's surface. Due to geological anomalies in certain places and in deep boreholes, the temperature differences to the surface are high enough to appropriate and technically convert in *geothermal power* plants.

Last but not least, an even smaller energy flux of about 3×10^{12} W fed from rotational inertia of the gravitationally coupled earth–moon–sun system enters the Earth system [4,8]. Tidal forces mainly from the orbiting moon combined with the Earth's rotation lead to a periodic lift of ocean water. The available energy potential in tides can be appropriated and converted to technical energy in *tide power* plants.

Each conversion process in the cascaded Earth system (e.g., solar irradiance $\rightarrow$ evaporation $\rightarrow$ precipitation $\rightarrow$ surface runoff) has a limited thermodynamic efficiency and reduces the appropriable potential of the resulting RE resources significantly [1]. The fewer conversion steps, the more of the initial energy is available for technical conversion, and thus, the higher the possible yield.

Table S1. Comparison of theoretical and appropriable technical potentials (ATPs) used in this study. The theoretical potential is indicated here as the value corresponding to each renewable energy (RE) resource; conversion in the Earth system is not accounted for. Consequently, the individual entries in this column do not add up to the total theoretical potential.

RE resource	technology	theoretical potential P_{th} / TW	appropriable potential P_{app} / TW	final RE potential P_{el} / TW
wind onshore	wind turbine	243	12	0.134
wind offshore	wind turbine	611	2	0.12
wave	WEC	56.7	0.18	0.02
ocean temperature gradient	OTEC	3.42	0.034	0.0045
salinity gradient	forward osmosis	3.02	0.016	0.014
freshwater runoff	hydro turbine	4.9	0.47	0.43
ocean NPP	combustion	69.6	0	0
forest NPP	combustion	101	0.63	0.143
agricultural NPP	combustion	16.5	0	0
solar on infrastructure	PV	20036	559	20.9
solar on desert	PV / CSP	2334	924	49
tides	hydro turbine	2.85	0.029	0.0067
terrestrial heat	geothermal power	29.45	8.4	0.3
total		172947	1507	71

2. Uncertainty Modeling

Each parameter is modeled as an uncertainty distribution (see tab. S2). The error propagation throughout the calculation is considered with Monte Carlo simulations, i.e., calculations are run 100 000 times with randomly picked values as specified by the parameter's uncertainty distributions.

Since no uncertainties regarding the climax vegetation are indicated in the original publication [9], they are estimated here as normally distributed within the range of $3\,\sigma = \pm 1\,\%$. The resulting limits

Table S2. Distributions to calculate random numbers for Monte-Carlo simulations.

distribution	description	min	mode	max	d
beta-PERT	smooth PDF with absolute min and max	a	c	b	1
triangular	forms a triangle between $(min, p = 0), (mode, p(mode)), (max, p = 0)$ with $p(mode)$ so that $\int_{min}^{max} p = 1$	a	c	b	2
normal	Gaussian distribution	-	μ	$\mu + 3\sigma$	3
log-normal	ln-transformed Gaussian distribution	-	e^{μ}	$e^{\mu+3\sigma}$	4
uniform	each value between min and max has the same probability	min	-	max	5
balance coefficient	is determined as the residue to 1 for columns in a matrix. Only relevant, if the sum of each column in a matrix needs to equal 1	-	-	-	6

to appropriate land from the different biomes are given as minimum and maximum values without information about the distribution [10]. Therefore, a rectangular distribution is assumed.

3. Electric Energy Conversion Efficiency

In energy statistics of the international energy agency (IEA), primary energy use is reported on the level of caloric energy content of fuels for some energy carriers (e.g., oil) and electricity for others (e.g., solar) [11]. The same applies to the life cycle inventory database ecoinvent [12] and other databases. In order to convert these energy flows to the common form of electric energy, average conversion factors are applied (see table S3) [13]. For specific RE technologies, the conversion efficiency is described in the respective section in this Supplementary Material.

Table S3. Average conversion efficiency of different energy carriers into electric energy [13].

Conversion of energy carrier into electric energy	conversion efficiency [13]
Biomass	0.25
Natural gas	0.4
Oil	0.37
Coal	0.34
Uranium	0.33

4. Applied Land Use Scenarios

The land system change boundary specifies the maximum land area appropriable for human use. It is segmented in three land use types: cropland, pasture, and built environment. Cropland, including forest plantations (e.g., oil palms), is required to feed humanity and nongrazing livestock but also needs to satisfy nonfood agricultural demand (e.g., fibers, timber, agrofuels). Pasture is used for the grazing of domestic animals. Built environment includes all other surfaces changed by humans (e.g., buildings, roads, mines). The following three exemplary segmentation scenarios (see also Figure S3) are investigated in this study:

1. *Proportional*: The land use mix is divided according to actual data on biome resolution in the year 2000 [14–20]. For each biome, the appropriable land is allocated according to its relative share in 2000. Infrastructure data are available as the global average only, which is applied evenly over all biomes. In some biomes (e.g., tropical forest), land use exceeds safe limits in 2000 and is therefore reduced accordingly. In other biomes (e.g., temperate forest), the opposite is the case. Overall, this scenario yields global areas for each land use type lying between the aggregated values for the years 2000 and 2010 [21,22];

2. *Reduce pasture*: Pasture is seen as an additional source of food and not essential for human survival [23]. Therefore, the area of cropland and infrastructure is kept at the level of 2010 and pasture is rescaled to fit the PB. It is assumed that the increase in cropland (+20 %) and infrastructure (+3 %) from 2000 to 2010 was shared equally across all biomes. In the *tropical forest*, the cropland area exceeds the appropriable area; therefore, its fraction is limited to 90 %. In deserts, we assume that pasture and cropland remain constant at 2010 level as NPP is low, leaving the rest for infrastructure. The reference for the calculation is the 1 %-quantile of the distribution of appropriable land (see Figure S3);
3. *Maximize cropland*: To increase the food supply for a growing population [24], the cropland area is increased in this scenario [23]. The built environment is kept as in scenario 2, while pasture area is reduced. It is assumed that cropland areas can be increased on areas where the climax vegetation would be forest by 50 % and on areas which would be savannas, grasslands/steppe and shrub land/tundra biomes by 25 % relative to scenario 2. As cropland on tropical forest areas has already surpassed the appropriable limit, it is kept at 90 %. Further, cropland and pasture in deserts remain as in scenario 2.

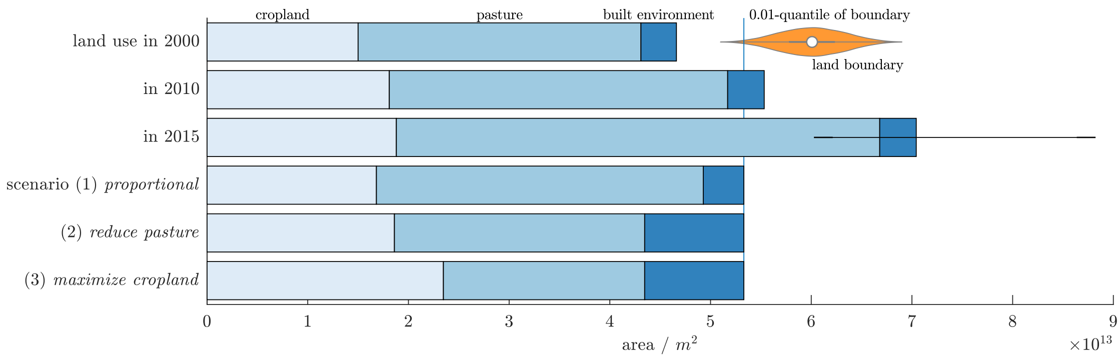

Figure S3. Different land use scenarios (1–3) and historic land use data (2000 [14,18,19,25], 2010 [21,22], 2015 including uncertainty (min, max) [19,26]), divided into cropland, pasture, and built environment, in comparison with the land system change boundary [10,27].

These land use scenarios define the area available for technical energy conversion. Therefore, each land use type can be used for multiple purposes simultaneously, e.g., pasture for grazing and wind energy conversion or built environment for housing and solar energy conversion. However, as argued in the main text, whenever technical energy conversion competes with chemical energy demand, the latter is given priority (e.g., solar energy conversion on cropland is not permitted).

5. Data and Assumptions Used to Calculate ATPs

5.1. Solar

The highest overall efficiency can be obtained by converting solar irradiance into electric energy [28]. Two main conversion technologies (photovoltaic (PV) and concentrated solar power (CSP)) are currently available. The decisive limiting factor for direct solar energy conversion is the appropriable surface area. According to the PB, appropriation of surface is limited to about 2/5 of the total land area (see main text). Water surface is not restricted in the PB; however, the effects of large scale coverage of ocean and lake surfaces on weather systems, marine life, and fisheries are currently unknown. In addition to that, technical solutions are currently unavailable. Consequently, water surfaces are not appropriable in this assessment. Most of the appropriable land surface is necessary to satisfy human demand for chemical energy, such as food, feed or fiber (see Section 4). Built environment surfaces and low NPP land such as deserts are therefore the only appropriable surfaces for direct solar energy conversion. The built environment subdivides into buildings, roads, parking, rail networks, gardens, green belts, and others. On buildings, the entire envelope, i.e., roof and facade areas exposed to direct and diffuse irradiance is potentially usable for harvesting solar potential. This area approximately matches the area of the covered surface. However, not all building envelopes are suitable for PV systems: They might be shaded by taller buildings, mountains or trees or are historically important and cannot be changed. Globally, approximately 18 % of the built environment is covered by buildings in 2000 and 21 % in 2015 [18,19,25,26,29]. As the density of buildings in built environments is increasing, we assume an interval for the building fraction of $[0.21, 0.25]$. In Switzerland, about 60 % of roof area is estimated to be suitable for PV systems [30]. In the US, this value is between 70 % to 80 % [31]. Additionally, facades can be utilized, and for Switzerland, it is estimated that the suitable facade area corresponds to about 40 % of covered surface area (= roof area), though with roughly 1/3 of the energy yield of a roof PV system. For locations closer to the equator with a higher solar altitude, this value is smaller and vice versa. In this study, we estimated the globally available energy potential of buildings to between 70 % and 80 % of the PV potential of the covered surface.

Roads, open parking spaces, rail tracks, and similar uses seal 18 % to 20 % of the built environment [18,19,25,26,29]. This area can potentially be used for solar power conversion, though to a lesser extent and with added technical difficulties. We estimate that globally, 20 % to 50 % of this area is available for PV conversion. All other covered surfaces are excluded. In total, we therefore estimate that 18 % to 30 % of the projected surface area of the built environment can convert solar irradiance to electric energy with PV technologies.

The desert area is largely unsuitable for agriculture or animal husbandry [32]; therefore, large surfaces could be available for infrastructures. The effect of covering large desert areas with solar technology on weather patterns, albedo, and wildlife is currently unknown and would need to be assessed in detail. Further, the built environment in deserts may have multiple competing usages, such as mining or roads. Therefore, not the entire built environment in deserts is available for solar power conversion. We estimate the appropriable area suitable for solar technologies to be in the range of 20 % (similar to other built environments) to 80 % (limited by geometry, e.g., of access paths).

The yield of a solar energy system depends, among other factors, on the location on the Earth's surface. Locations closer to the equator have a higher irradiance and potentially higher yields. This dependence is modeled with a simple geometric relationship between the slice of the cross-section of a sphere and its corresponding surface (Equation 1). For the different biomes, the irradiance is divided according to the latitude range of the biome (taken from [33]). A simple geometrical relationship between the cross-section, which receives a constant irradiance, and the surface ring of the sphere is made.

$$f_{\text{irr}}(\phi_1, \phi_2) = \frac{\int_{\phi_1}^{\phi_2} dA_{\text{cross section}}}{\int_{\phi_1}^{\phi_2} dA_{\text{surface}}} = \frac{\int_{\phi_1}^{\phi_2} 2r^2 \cos^2 \phi d\phi}{\int_{\phi_1}^{\phi_2} 2\pi r^2 \cos \phi d\phi} = \frac{\phi_2 - \phi_1 + \sin\phi_2 \cos\phi_2 - \sin\phi_1 \cos\phi_1}{2\pi(\sin\phi_2 - \sin\phi_1)} \tag{1}$$

For the entire sphere, this factor is $f_{\text{irr}}(-90\,^\circ, 90\,^\circ) = 0.25$ (circle area to sphere surface with same radius); for areas closer to the equator, the factor is higher, while for areas closer to the poles smaller. The solar irradiance, which is received by the Earth's surface, is mapped on the different biome types accounting for the geometric differences on their location on Earth.

Other factors are local weather patterns or ambient temperature. A comparison to other studies [30,31,34–36], which model solar yields for specific locations and regions using GIS data on irradiance and local conditions (e.g., roof topography), shows that local factors other than position are of minor importance when integrating over large areas. The error is $< \pm 4\,\%$ for regions like the entire United States [31] or Switzerland [30]. Thus, these are of minor influence for a global assessment and therefore not considered. For smaller regions with specific conditions (e.g., Arizona in the US with low precipitation [31]), deviation increases significantly up to 25 %. A spatially explicit global assessment could be integrated to refine the results in the future.

Photovoltaic systems (PV) convert direct and diffuse irradiance into electric power without moving parts (solid state). Depending on location and module orientation, some of the irradiance is lost due to reflection ($\gamma_{\text{refl.}} = [0.025, 0.06]$ [34]). The module efficiency ranges between $\eta_{\text{PV,module}} = [0.17, 0.4]$ [30,31,34,37,38] under standard test conditions (STC: 1000 W/m², 25 °C [38]). Losses may occur by deviating STC (temperature and irradiance $\gamma_{\text{temp.}} = [0.02, 0.11]$ [34]), and some electrical system losses (e.g., in inverters and cables) in the range of $\gamma_{\text{el},p=1} = 0.14^{+0.06}_{-0.04}$ [34] are inevitable.

Concentrated solar power (CSP) systems convert irradiance first into high temperature heat and, in a second step, into electric power via heat engines. Individual CSP systems require large areas and are not easily integrated into buildings. Therefore, this technology is currently only viable in deserts. Current annual average efficiencies are in the range of $\eta_{\text{CSP}} = [0.1, 0.3]$ and thus lower than PV systems [38]. Therefore, it is assumed that only large scale CSP systems will be installed, once they reach a higher efficiency.

Appropriable solar potential on desert surfaces is estimated with PV system performance. The losses due to reflection as well as temperature and low irradiance are slightly smaller in desert areas than on average [34]; therefore, the overall efficiency of PV systems is modeled as slightly higher (see Excel calculation sheet for more details).

5.2. Hydro Power and Power from Forward Osmosis

The global water cycle transports water vapor from ocean to land surfaces, where precipitations result in a runoff of surface freshwater back to the oceans of 1.46×10^6 m³/s [7]. This runoff has a geodetic potential of 5×10^{12} W [4,39] and a mixing free energy of freshwater with seawater of 2.9×10^6 J/m³ [40], a total potential for the salinity gradient of 4.24×10^{12} W.

In 2011, non-energy sectors required 2.3×10^4 m³/s of the run-off [41]. Assuming this demand is constant, the remainder to the PB (see main text) can be appropriated for electric power generation, which is in the case of an all-renewable scenario hydro and forward osmosis (FO) [1]. The appropriable limit is therefore $[0.11, 0.74] \times \dot{V}_{\text{global}}$. It is assumed that $[0.90, 0.95]$ of the appropriable potential is converted by hydro power plants, and the rest by FO.

Biodiversity impacts can be technically minimized through fish ladders and specific hydraulic design in state-of-the-art technology [42]; however, they are technology-specific and therefore not considered in this study. Conversion efficiency in hydro power plants is reduced by losses in ducts ($\eta_{\text{ducts}} = [0.9, 0.98]$ [38,39]), turbines ($\eta_{\text{turbine}} = [0.85, 0.96]$ [39,43]) and electrical installations ($\eta_{\text{el}} = [0.95, 0.98]$ [39]).

When freshwater meets the ocean, the mixing free energy is dissipated as low temperature heat. FO with a conversion efficiency of $\eta_{\text{FO}} = [0.4, 0.48]$ can be applied to utilize this energy potential [40]. River deltas are fragile ecosystems, and the water flow is often spread out over huge areas, posing a logistical challenge in capturing this resource's potential. It remains to be estimated how FO impacts biodiversity both up and downstream.

5.3. Wind and Wave

Wind is largely created by temperature differences in the atmosphere with an energy potential of approximately 9×10^{14} W globally [1,39,44]. About half of this potential is dissipated in the $\delta = [900, 1000]$ m thick atmospheric boundary layer [44] between surface and free atmosphere [5]. In the boundary layer, the horizontal velocity v_x increases logarithmically with altitude z [5]:

$$v_x(z) = \frac{u_*}{\kappa} \ln \frac{z}{z_0} \tag{2}$$

[1] The reversal of the process (reverse osmosis, RO) is used for desalination.

with surface tension velocity $u_* = \sqrt{\frac{\tau_w}{\rho}}$ [45], the Kármán constant $\kappa = 0.4$, and the surface roughness height z_0, depending on the surface type [5]. The wind power is a function of area perpendicular to wind direction x, density of air ρ, and wind velocity v_x:

$$dP(z) = \frac{\rho}{2} \cdot dy \cdot dz \cdot v_x^3(z) \tag{3}$$

$$P_{\text{boundary}} = \frac{\rho u_*^3}{2\kappa^3} \cdot l_y \int_0^\delta \left(\ln \frac{z}{z_0}\right)^3 dz \tag{4}$$

Wind turbines have technological restrictions in size, with a hub-height of $H = [80, 170]$ m [39,46,47] and a diameter of $D = [80, 250]$ m [39,47]. Generally, offshore turbines are slightly larger than onshore [39]; therefore, the respective intervals for offshore turbines are assumed to start with $H = D = 100$ m. The range reflects the current technological average up to future potential [47]. The wind turbine parameters determine the fraction of the boundary layer volume, where technical energy conversion is possible.

Wind power extraction is only possible in the range of the rotor from $z_l = H - \frac{D}{2}$ to $z_u = H + \frac{D}{2}$, and thus, the fraction of wind power that can be extracted from the boundary layer is:

$$f_{\text{WT/BL}} = \frac{\int_{z_l}^{z_u} \left(\ln \frac{z}{z_0}\right)^3 dz}{\int_0^\delta \left(\ln \frac{z}{z_0}\right)^3 dz} \tag{5}$$

This fraction is a function of surface roughness only. For offshore areas, the surface roughness is $z_0 = [0.001, 0.02]$ m [5] and for onshore, it is assumed that wind parks would preferably be installed on pastures, cropland, and other similarly smooth areas, which results in $z_0 = [0.01, 0.2]$ m [5].

Wind parks can be installed on land as well as offshore. Offshore wind parks need to be close to the shoreline, due to maintenance access, increased sea roughness, cable length, link to sea floor, and other reasons. On average, wind parks can be installed within $l_{p=1} = 43.3^{+57}_{-33}$ km from shore [48]. Furthermore, it is assumed that between 30 % and 80 % of this area can be populated with wind parks, leaving enough surface for shipping routes, access to ports, coastal fisheries, etc. [49]. Onshore, the occupation of land is marginal (i.e., the tower cross-section); however, it creates obstacles for farming, visual obstruction, and noise. Therefore, it is assumed that a maximum of 20 % to 40 % of cropland and pastures can be used for wind farms, with the exception of former forest biomes. Because of the surrounding forest, the wind speeds close to the surface are low, which in turn makes it technically unsuitable, and the wind turbine fraction is set to zero. The built environment surfaces are unsuitable due to high surface roughness [5] and noise. The impacts on biodiversity (collision of birds with blades, noise, impact on food web [49]) are not considered in this study.

Wind turbines can harvest a theoretical maximum of 59 % of the kinetic power in the wind, which is known as the Betz' limit [39,44]. Achievable aerodynamic efficiency is somewhat lower between 40 % and 50 %, and additional losses in the mechanical and electrical system amount to 5 % to 15 % [39].

Waves are mainly caused by shearing forces between wind and the ocean surface. The wave energy potential amounts to approximately 7 % of wind energy or 6.3×10^{13} W [1]. Practically possible wave parks are restricted to coastal ocean surfaces with enough wind, which is estimated to have an appropriable potential along suitable coast lines of 2.11×10^{12} W [50]. Wave energy conversion (WEC) devices have to be sufficiently spaced due to operational requirements, which limits the technical potential to 0.046 of the coastal potential [50]. It is assumed that WEC parks can be installed at $[0.3, 0.5]$ of the total coast line, due to access to ports, coastal fisheries, recreational areas, and protected areas (e.g., coral reefs). A typical efficiency for WEC devices ranges $\eta_{\text{WEC}} = [0.2, 0.5]$, depending on the technology [51,52].

5.4. Terrestrial heat

Net heat flux from the Earth's interior to the surface is 3×10^{13} W [4,53,54] Its origins are radioactive decay, crystallization, and residual heat. Areas with a heat gradient larger than 0.1 K/m are suitable for geothermal power conversion [53], which is mainly the case in geological anomalies [54]. It is assumed that the heat flux is evenly distributed on the planet but that geothermal power cannot be harvested on ocean floors, restricting the accessible potential to land only. It is estimated that $[0.1, 0.3]$ of the theoretical heat flux can be appropriated. Typical upper $T_{\text{max}} = [443, 543]$ K and lower process temperatures $T_{\text{min}} = [303, 313]$ K[53] result in a Carnot efficiency:

$$\eta_{\text{C}} = 1 - \frac{T_{\text{min}}}{T_{\text{max}}} \tag{6}$$

Depending on the technology used, practically achievable efficiencies are $[0.8, 0.9]$ of the Carnot efficiency [38].

5.5. Biomass Production

5.5.1. Agriculture

The main purpose of agriculture is to produce food. As outlined in the main text, food production systems face the challenge of feeding a growing human population and are already breaching Earth system boundaries. Therefore, dedicated agrofuel production is not considered.

Other potential resources of agricultural origin are food waste and harvest residues. Food waste should be reduced as much as possible [55–57], leaving the option to harvest residues [58]. To estimate whether residues from agriculture could potentially be important as a technical energy resource, we considered the total useful harvest of NPP for food (1.3×10^{12} W in the year 2000 [59]) and fodder (4×10^{12} W) in relation to the direct HANPP. A bit more than 1/3 of the direct HANPP is not utilized as food or fodder and is left as, e.g., harvest residues or feces [59]. Considering that 50 % of the chemical energy potential can be converted to electric energy with an efficiency of 30 %, a technical potential of 3×10^{11} W would become available. Daioglou and colleagues [58] arrive at a similar value by considering agricultural residues without the fraction considered necessary to maintain soil quality, animal feed, and traditional fuel. However, the authors emphasize that the mechanisms to maintain soil quality are largely unclear and therefore uncertain [58]. Moreover, the study does not consider Earth system boundaries, and it remains unquestioned if a change in agricultural practice, in order to respect Earth system boundaries, would not change the availability of residues in return. In our view, an evaluation of agricultural residues would require evaluating agricultural practice against Earth system boundaries and future food demand. Only then will it be possible to evaluate whether or not the agricultural sector can provide technical energy in addition to fulfilling the chemical energy demand.

5.5.2. Forestry

In forest areas, wood for material and energetic use can be harvested given sustainable forest management is in place [21,60]. Parts of the forest area are not accessible for appropriation, due to protected habitats or geographical remoteness (e.g., mountain regions). Today, (13 % of forests is protected [21] and 36 % is still primary forest and probably worth protecting [21]. A total of 50 % is argued to need protection to maintain biodiversity [27]) and the regeneration of the forest ecosystem [21].

The sustainable harvest rate of the net annual increment $NAI = [1.9, 3.5] \times 10^{-4}$ m³/m²·a is between 60 % and 80 % on the accessible and nonprotected forest area [21].

The harvested wood is assumed to enter a cascaded use where, finally, all chemical energy is used for conversion to electric energy (e.g., via a conventional combustion process and Rankine cycle or pyrolysis and combustion in a internal combustion engine or gas turbine). We assume a conversion efficiency of $\eta_{p=1} = 0.35^{+0.05}_{-0.15}$ [38,61].

5.5.3. Marine biomass production

Algae and phytoplankton are the basis of the trophic chain in the oceans [62]. The ocean's food web is already under great pressure [63] to provide for current food supply (i.e., aquaculture and wild catch). The consequences of appropriating additional ocean biomass for technical energy supply are largely unclear [61,63] and in competition with food production. Therefore, this RE potential is excluded from the assessment.

5.6. Tides

The gravitationally coupled motion of the earth–moon–sun system accelerates ocean waters by tidal forces, which excites the water to slosh periodically in the ocean basins producing sea level changes known as tides. The energy dissipated in ocean tides is estimated at 3×10^{12} W [4,8]. Most of this energy is dissipated at the rising sea floor between open ocean and shore [8]. Tidal power can be harvested using the sea level difference or tidal currents in channels. Technically feasible power conversion, however, requires coastal areas with sufficiently high sea level differences and suitable geography (i.e., channels, bays, ...), which are estimated to be $[0.01, 0.05]$ of the total coast line. Furthermore, it is estimated that $[0.2, 0.3]$ of the total energy is dissipated at the shoreline, whereas the rest is dissipated as friction at the rising ocean floor and in the water itself [8]. The energy can be converted with conventional hydro turbines (see Section 5.2).

5.7. Ocean thermal energy conversion

The ocean surface water in the tropics has a temperature between $[25, 30]$ °C, which is sufficiently higher than temperatures in 1000 m depth of about $[4, 7]$ °C in order to drive a heat engine and convert the energy flux into electric energy. The theoretical potential is estimated as approximately 6.85×10^{12} W [61,64]. The Carnot efficiency (Equation 6) is, however, low due to the small temperature difference [53]. Increasing the temperature in deep water reduces the solubility of CO_2. Therefore mixing heat of surface to deep water eventually releases CO_2 into the atmosphere. Additionally, the accessible area can only be accessed partly, due to geometric parameter, such as distance to shore, access to ports, area required for local fisheries, etc. We therefore assume that $[0.01, 0.05]$ of the area with suitable temperature differences can actually be covered with heat exchange devices. A more rigorous assessment would need to quantify the impact of CO_2 release on the climate boundary.

6. Glossary and acronyms

The following terms are used in this manuscript.

term	**description**
ATP	Appropriable technical potential is the energy flux appropriable for society in the form of electric energy that can be produced with state-of-the-art technology after subtracting the appropriable chemical potential and respecting Earth system boundaries. It is the appropriable potential minus what is needed to provide the appropriable chemical potential, plus the energy that can be recovered as technical energy from chemical use and minus technical conversion losses.
Accessibility	Can be reached for human appropriation.
Appropriability	That can be appropriated.

term	description
To appropriate	Taking something that belongs to someone else usually without having the right to do so.
Availability	The fact that something can be used, or utilized (e.g., by the Earth system or humanity).
Built environment	Surfaces dominated by settlements, infrastructure, mining, etc. This includes parks, gardens, green belts along with infrastructure area.
Built-up area	Ground area of spatial units containing buildings or parts thereof [20].
Circular economy	The circular economy is a model adopting a resource-based and systemic view, aiming at taking into account all the variables of the system Earth, in order to maintain its viability for human beings. It serves the society to achieve well-being within the physical limits and planetary boundaries. It achieves that through technology and business model innovation, which provide the goods and services required by society, leading to long-term economic prosperity. These goods and services are powered by renewable energy and rely on materials which are either renewable through biological processes or can be safely kept in the technosphere, requiring minimum raw material extraction and ensuring safe disposal of inevitable waste and dispersion in the environment. CE builds on and manages the sustainably available resources and optimizes their utilization through minimizing entropy production, slow cycles, and resource and energy efficiency [65].
Chemical energy	Chemical energy is understood as the energy used to supply humanity with food and biogenic materials (fodder, fibers, timber, etc.).
Climax vegetation	Equilibrium vegetation that would be reached according to environmental parameter (e.g., temperature, humidity) if undisturbed.
Earth system	The entirety of the Earth's interacting physical, chemical, and biological processes.
Earth system boundaries	Limits to Earth system processes that, if crossed, significantly disturb the interacting web of processes with potential to trigger fast and irreversible change to a new equilibrium.
Earth system needs	Energy and material flows that are required by Earth system processes to maintain functionality.
Energy	The cumulative flux, i.e.. its integral over a given period of time.
Exergy	The useful work that can be extracted from an energy flow.
Flux	The surface integral of the orthogonal component of the flux density. It represents, e.g., the em power emitted, reflected, transmitted or received by this surface. The same term and procedure is also used for non-energy quantities, e.g., magnetic flux. In other disciplines, "flow" is the preferred and synonymous term, e.g., mass flow.

term	description
Flux density	In the context of em radiation, the vector field "flux density" refers to the directed power emitted, reflected, transmitted or received by an infinitesimal surface. Here, we adhere to radiometric SI terms and units.
HANPP	Human appropriation of NPP comprises direct harvest (e.g., food production, timber) and human induced changes in productivity (e.g., land use change, fire) [59].
Infrastructure surface	Built-up plus other sealed surfaces, such as roads, railways, airports, bridges, etc.
Irradiance, solar	Consists of electromagnetic radiation (i.e., photon flux) of solar origin.
Radiation, solar	Consists of photon flux and particle flux i.e. electromagnetic (em) waves and solar wind (i.e., particles such as electrons and protons).
NPP	Net primary production [59].
Prospective technology	Lab-scale, prototype or pilot systems that have not proven successful in the market yet.
Planetary boundaries	A “safe operating space” within which changes in nine planetary processes (stratospheric ozone depletion, nitrogen/phosphorus cycle change, global freshwater use, land use change, biodiversity loss, atmospheric aerosol loading, chemical pollution, climate change, and ocean acidification) must remain to avoid the risk of setting off a cascade of irreversible change.
(RE) potential, theoretical	The available (RE) flux in the Earth system (replace (RE) with any RE type or combinations thereof). For example, the NPP potential is the calorific value of the net primary production. For the total incoming energy, it is the sum of the three energy flows entering the Earth system (solar, geothermal, tides), i.e.. approximately 174000 TW
(RE) potential, appropriable	The appropriable fraction of the theoretical (RE) potential, i.e., the theoretical (RE) potential minus Earth system needs. For example, the appropriable NPP potential is the Earth’s entire climax NPP minus the minimum NPP required to respect Earth system boundaries.
State-of-the-art technology	widely used technology, available in the market in various different products.

References

1. Kleidon, A. Thermodynamik des Erdsystems - Was leistet die Erde? *Physik unserer Zeit* **2012**, *3*, 136–144. www.doi.org/10.1002/piuz.201201294.
2. Szargut, J.T. Anthropogenic and natural exergy losses (exergy balance of the Earth’s surface and atmosphere). *Energy* **2003**, *28*, 1047–1054. www.doi.org/10.1016/s0360-5442(03)00089-6.
3. Potter, T. Handbook of weather, climate, and water : dynamics, climate, physical meteorology, weather systems, and measurements / edited by Thomas D. Potter, Bradley R. Colman Handbook of Weather, Climate and Water. *Handbook of Weather, Climate and Water* **2003**.
4. Chen, G.Q. Exergy consumption of the earth. *Ecological Modelling* **2005**, *184*, 363–380. www.doi.org/10.1016/j.ecolmodel.2004.10.015.
5. Roedel, W.; Wagner, T. *Physik unserer Umwelt - Die Atmosphäre*, 4 ed.; Springer, 2011. www.doi.org/10.1007/978-3-642-15729-5.

6. L'Ecuyer, T.; Beaudoing, H.K.; Rodell, M.; Olsen, W.; Lin, B.; Kato, S.; Clayson, C.; Wood, E.; Sheffield, J.; Adler, R.; Huffman, G.; Bosilovich, M.; Gu, G.; Robertson, F.; Houser, P.; Chambers, D.; FAMIGLIETTI, J.; Fetzer, E.; Liu, W.; Gao, X.; Schlosser, G.; Clark, E.; Lettenmaier, D.; Hilburn, K. The Observed State of the Energy Budget in the Early Twenty-First Century. *Journal of Climate* **2015**, *28*, 8319–8346. www.doi.org/10.1175/JCLI-D-14-00556.1.
7. Rodell, M.; Beaudoing, H.K.; L'Ecuyer, T.; Olsen, W.; FAMIGLIETTI, J.; Houser, P.; Adler, R.; Bosilovich, M.; Clayson, C.; Chambers, D.; Clark, E.; Fetzer, E.; Gao, D.; Gu, G.; Hilburn, K.; Huffman, G.; Lettenmaier, D.; Liu, W.; Robertson, F.; Schlosser, G.; Sheffield, J.; Wood, E. The Observed State of the Water Cycle in the Early Twenty-First Century. *Journal of Climate* **2015**, *28*, 8289–8310. www.doi.org/10.1175/JCLI-D-14-00555.1.
8. Accad, Y.; Pekeris, L. Solution of the tidal equations for the M2 and S2 tides in the worlds oceans from the knowledge of the tide potential alone. *Philosophical Transactions of the Royal Society a-Mathematical Physical and Engineering Sciences* **1978**, *290*, 235–266.
9. Ramankutty, N.; Foley, J.A. Estimating historical changes in global land cover: croplands from 1700 to 1992. *Global Biochemical Cycles* **1999**, *13*, 997–1027. www.doi.org/10.1029/1999GB900046.
10. Steffen, W.; Richardson, K.; Rockstrom, J.; Cornell, S.E.; Fetzer, I.; Bennett, E.M.; Biggs, R.; Carpenter, S.R.; de Vries, W.; de Wit, C.A.; Folke, C.; Gerten, D.; Heinke, J.; Mace, G.M.; Persson, L.M.; Ramanathan, V.; Reyers, B.; Sorlin, S. Sustainability. Planetary boundaries: guiding human development on a changing planet. *Science* **2015**, *347*, 1259855. www.doi.org/10.1126/science.1259855.
11. International Energy Agency. Energy Balance for the World, 2015, 2018. https://www.iea.org/Sankey/#?c=World&s=Balance.
12. Wernet, G.; Bauer, C.; Steubing, B.; Reinhard, J.; Moreno-Ruiz, E.; Weidema, B. The ecoinvent database version 3 (part I): overview and methodology. *The International Journal of Life Cycle Assessment* **2016**, *21*, 1218–1230. www.doi.org/10.1007/s11367-016-1087-8.
13. Cullen, J.M.; Allwood, J.M. Theoretical efficiency limits for energy conversion devices. *Energy* **2010**, *35*, 2059–2069. www.doi.org/10.1016/j.energy.2010.01.024.
14. Ramankutty, N. Farming the planet: 1. Geographic distribution of global agricultural lands in the year 2000. *Global Biochemical Cycles* **2008**, *22*, 1–19. www.doi.org/10.1029/2007GB002952.
15. Monfreda, C.; Ramankutty, N.; Foley, J.A. Farming the planet: 2. Geographic distribution of crop areas, yields, physiological types, and net primary production in the year 2000. *Global Biochemical Cycles* **2008**, *22*, 1–19. www.doi.org/10.1029/2007GB002947.
16. Schneider, D. *Quantitative Ecology*; Academic Press, 2009. www.doi.org/https://doi.org/10.1016/C2009-0-02446-5.
17. Center for International Earth Science Information Network, Ciesin Columbia University and International Food Policy Research Institute, Ifpri and The World, Bank and Centro Internacional de Agricultura Tropical, Ciat. Global Rural-Urban Mapping Project, Version 1 (GRUMPv1): Urban Extents Grid, 2011. https://doi.org/10.7927/H4GH9FVG.
18. Erb, K.H.; Gaube, V.; Krausmann, F.; Plutzar, C.; Bondeau, A.; Haberl, H. A comprehensive global 5 min resolution land-use data set for the year 2000 consistent with national census data. *Journal of Land Use Science* **2007**, *2*, 191–224. www.doi.org/10.1080/17474230701622981.
19. Joint Research Center. Atlas of the human planet 2016 - Mapping Human Presence on Earth with the Global Human Settlement Layer. Report, JRC, 2016. www.doi.org/10.2788/889483.
20. Joint Research Center. Operating procedure for the production of the Global Human Settlement Layer from Landsat data of the epochs 1975, 1990, 2000, and 2014. Report, JRC, 2016. www.doi.org/10.2788/656115.
21. O'Brien, M. Timber consumption and sustainable forest use: Assessing the EU's current and expected consumption of global timber in relation to the global capacity for sustainable supply. Thesis, 2015.
22. World Bank. Land conversion data, 2018. https://data.worldbank.org/indicator/AG.LND.TOTL.K2.
23. Cassidy, E.S.; West, P.C.; Gerber, J.S.; Foley, J.A. Redefining agricultural yields: from tonnes to people nourished per hectare. *Environmental Research Letters* **2013**, *8*. www.doi.org/10.1088/1748-9326/8/3/034015.
24. United Nations Department of Economic and Social Affairs. World Population Prospects 2019: Highlights. Report ST/ESA/SER:A/423, United Nations, 2019. https://population.un.org/wpp/Publications/.
25. Schneider, A.; Friedl, M.A.; Potere, D. A new map of global urban extent from MODIS satellite data. *Environmental Research Letters* **2009**, *4*. www.doi.org/10.1088/1748-9326/4/4/044003.

26. IPCC. IPCC Special Report on Climate Change, Desertification, Land Degradation, Sustainable Land Management, Food Security, and Greenhouse gas fluxes in Terrestrial Ecosystems. Report, 2019.
27. Dinerstein, E.; Olson, D.; Joshi, A.; Vynne, C.; Burgess, N.D.; Wikramanayake, E.; Hahn, N.; Palminteri, S.; Hedao, P.; Noss, R.; Hansen, M.; Locke, H.; Ellis, E.C.; Jones, B.; Barber, C.V.; Hayes, R.; Kormos, C.; Martin, V.; Crist, E.; Sechrest, W.; Price, L.; Baillie, J.E.M.; Weeden, D.; Suckling, K.; Davis, C.; Sizer, N.; Moore, R.; Thau, D.; Birch, T.; Potapov, P.; Turubanova, S.; Tyukavina, A.; de Souza, N.; Pintea, L.; Brito, J.C.; Llewellyn, O.A.; Miller, A.G.; Patzelt, A.; Ghazanfar, S.A.; Timberlake, J.; Kloser, H.; Shennan-Farpon, Y.; Kindt, R.; Lilleso, J.B.; van Breugel, P.; Graudal, L.; Voge, M.; Al-Shammari, K.F.; Saleem, M. An Ecoregion-Based Approach to Protecting Half the Terrestrial Realm. *Bioscience* **2017**, *67*, 534–545. www.doi.org/10.1093/biosci/bix014.
28. Kleidon, A.; Miller, L.; Gans, F., Physical Limits of Solar Energy Conversion in the Earth System. In *Solar Energy for Fuels*; Tuysuz, H.; Chan, C.K., Eds.; Springer International Publishing Ag: Cham, 2016; Vol. 371, *Topics in Current Chemistry-Series*, pp. 1–22. www.doi.org/10.1007/128_2015_637.
29. (BFS), Bundesamt für Statisitk. Die Bodennutzung in der Schweiz. Report, Sektion Geoinformation, BFS, 2013.
30. Klauser, D. Solarpotentialanalyse für Sonnendach.ch - Schlussbericht. Report, Bundesamt für Energie, 2016.
31. Gagnon, P.; Margolis, R.; Melius, J.; Phillips, C.; Elmore, R. Estimating rooftop solar technical potential across the US using a combination of GIS-based methods, lidar data, and statistical modeling. *Environmental Research Letters* **2018**, *13*. www.doi.org/10.1088/1748-9326/aaa554.
32. United Nations Environmental Program. Global Desert Outlook. Report, UNEP, 2006.
33. Snyder, P.K.; Delire, C.; Foley, J.A. Evaluating the influence of different vegetation biomes on the global climate. *Climate Dynamics* **2004**, *23*, 279–302. www.doi.org/10.1007/s00382-004-0430-0.
34. Joint Research Center. PV GIS tool, 2018. http://re.jrc.ec.europa.eu/pvg_tools/en/tools.html.
35. Gagnon, P.; Margolis, R.; Melius, J.; Phillips, C.; Elmore, R. Rooftop Solar Photovoltaic Technical Potential in the United States: A detailed Assessment. Report, National Renewable energy laboratory, 2016.
36. Campos, P.; Troncoso, L.; Lund, P.D.; Cuevas, C.; Fissore, A.; Garcia, R. Potential of distributed photovoltaics in urban Chile. *Solar Energy* **2016**, *135*, 43–49. www.doi.org/10.1016/j.solener.2016.05.043.
37. Fraunhofer Institut for Solar Energy Systems. Photovoltaics report. Report, Fraunhofer ISE, 2018. www.ise.fraunhofer.de.
38. Grote, K.; Feldhusen, J. *Dubbel - Taschenbuch für den Maschinenbau*, 21 ed.; Springer, 2005.
39. Schilling, R. Vorlesungskript Wasser- und Windturbinen, 2011.
40. Yip, N.; Elimelech, M. Thermodynamic and Energy Efficiency Analysis of Power Generation from Natural Salinity Gradients by Pressure Retarded Osmosis. *Environmental Science and Technology* **2012**, *46*, 5230–5239. www.doi.org/10.1021/es300060m.
41. Stadler, K.; Wood, R.; Bulavskaya, T.; Södersten, C.J.; Simas, M.; Schmidt, S.; Usubiaga, A.; Acosta-Fernández, J.; Kuenen, J.; Bruckner, M.; Giljum, S.; Lutter, S.; Merciai, S.; Schmidt, J.H.; Theurl, M.C.; Plutzar, C.; Kastner, T.; Eisenmenger, N.; Erb, K.H.; de Koning, A.; Tukker, A. EXIOBASE 3: Developing a Time Series of Detailed Environmentally Extended Multi-Regional Input-Output Tables. *Journal of Industrial Ecology* **2018**, *22*, 502–515. www.doi.org/10.1111/jiec.12715.
42. Rutschmann, P.; Sepp, A.; Geiger, F.; Barbier, J., Das Schachtkraftwerk – ein Wasserkraftkonzept in vollständiger Unterwasseranordnung. In *Wasserkraftprojekte*; Heimerl, S., Ed.; Springer, 2013; pp. 286–291. www.doi.org/10.1007/978-3-658-00996-0_37.
43. Sigloch, H. *Strömungsmaschinen*, 4 ed.; Carl Hanser, 2009.
44. Miller, L.M.; Gans, F.; Kleidon, A. Estimating maximum global land surface wind power extractability and associated climatic consequences. *Earth System Dynamics* **2011**, *2*, 1–12. www.doi.org/10.5194/esd-2-1-2011.
45. Adams, N. Fluidmechanik, 2011.
46. Miller, L.M.; Brunsell, N.A.; Mechem, D.B.; Gans, F.; Monaghan, A.J.; Vautard, R.; Keith, D.W.; Kleidon, A. Two methods for estimating limits to large-scale wind power generation. *Proceedings of the National Academy of Sciences of the United States of America* **2015**, *112*, 11169–11174. www.doi.org/10.1073/pnas.1408251112.
47. International Energy Agency. Technology Roadmap Wind Energy. Report, International Energy Agency,, 2013. www.iea.org.
48. European WInd Energy Association. The European offshore wind industry - key trends and statistics 2015. Report, EWEA, 2016. https://www.ewea.org/fileadmin/files/library/publications/statistics/EWEA-European-Offshore-Statistics-2015.pdf.

49. Bailey, H.; Brookes, K.L.; Thompson, P.M. Assessing environmental impacts of offshore wind farms: lessons learned and recommendations for the future. *Aquat Biosyst* **2014**, *10*, 8. www.doi.org/10.1186/2046-9063-10-8.
50. Gunn, K.; Stock-Williams, C. Quantifying the global wave power resource. *Renewable Energy* **2012**, *44*, 296–304. www.doi.org/10.1016/j.renene.2012.01.101.
51. Astariz, S.; Iglesias, G. The economics of wave energy: A review. *Renewable and Sustainable Energy Reviews* **2015**, *45*, 397–408. www.doi.org/10.1016/j.rser.2015.01.061.
52. Wu, B.; Li, M.; Wu, R.; Chen, T.; Zhang, Y.; Ye, Y. BBDB wave energy conversion technology and perspective in China. *Ocean Engineering* **2018**, *169*, 281–291. www.doi.org/10.1016/j.oceaneng.2018.09.037.
53. Zahoransky, R. *Energietechnik*, 4 ed.; Vieweh + Teubner, 2009.
54. Spliethoff, H. Renewable Energy Technology, 2012.
55. Foley, J.A.; Ramankutty, N.; Brauman, K.A.; Cassidy, E.S.; Gerber, J.S.; Johnston, M.; Mueller, N.D.; O'Connell, C.; Ray, D.K.; West, P.C.; Balzer, C.; Bennett, E.M.; Carpenter, S.R.; Hill, J.; Monfreda, C.; Polasky, S.; Rockstrom, J.; Sheehan, J.; Siebert, S.; Tilman, D.; Zaks, D.P. Solutions for a cultivated planet. *Nature* **2011**, *478*, 337–42. www.doi.org/10.1038/nature10452.
56. Willett, W.; Rockström, J.; Loken, B.; Springmann, M.; Lang, T.; Vermeulen, S.; Garnett, T.; Tilman, D.; DeClerck, F.; Wood, A.; Jonell, M.; Clark, M.; Gordon, L.J.; Fanzo, J.; Hawkes, C.; Zurayk, R.; Rivera, J.A.; De Vries, W.; Majele Sibanda, L.; Afshin, A.; Chaudhary, A.; Herrero, M.; Agustina, R.; Branca, F.; Lartey, A.; Fan, S.; Crona, B.; Fox, E.; Bignet, V.; Troell, M.; Lindahl, T.; Singh, S.; Cornell, S.E.; Srinath Reddy, K.; Narain, S.; Nishtar, S.; Murray, C.J.L. Food in the Anthropocene: the EAT–Lancet Commission on healthy diets from sustainable food systems. *The Lancet* **2019**, *393*, 447–492. www.doi.org/10.1016/s0140-6736(18)31788-4.
57. Shepon, A.; Eshel, G.; Noor, E.; Milo, R. The opportunity cost of animal based diets exceeds all food losses. *Proc Natl Acad Sci U S A* **2018**, *115*, 3804–3809. www.doi.org/10.1073/pnas.1713820115.
58. Daioglou, V.; Stehfest, E.; Wicke, B.; Faaij, A.; van Vuuren, D.P. Projections of the availability and cost of residues from agriculture and forestry. *GCB Bioenergy* **2016**, *8*, 456–470. www.doi.org/10.1111/gcbb.12285.
59. Haberl, H.; Erb, K.H.; Krausmann, F.; Gaube, V.; Bondeau, A.; Plutzar, C.; Gingrich, S.; Lucht, W.; Fischer-Kowalski, M. Quantifying and mapping the human appropriation of net primary production in earth's terrestrial ecosystems. *Proceedings of the National Academy of Sciences* **2007**, *104*, 12942. http://www.pnas.org/content/104/31/12942.abstract.
60. Krausmann, F.; Erb, K.H.; Gingrich, S.; Lauk, C.; Haberl, H. Global patterns of socioeconomic biomass flows in the year 2000: A comprehensive assessment of supply, consumption and constraints. *Ecological Economics* **2008**, *65*, 471–487. www.doi.org/10.1016/j.ecolecon.2007.07.012.
61. Intergovernmental Panel on Climate Change. Renewable Energy Sources and Climate Change Mitigation. Report, Intergovernmental Panel on Climate Change,, 2012.
62. Bar-On, Y.M.; Phillips, R.; Milo, R. The biomass distribution on Earth. *Proc Natl Acad Sci U S A* **2018**, *115*, 6506–6511. www.doi.org/10.1073/pnas.1711842115.
63. IPBES. Global assessment report on biodiversity and ecosystem services of the Intergovernmental Science-Policy Platform on Biodiversity and Ecosystem Services. Report, 2019.
64. Krewitt, W.; Nienhaus, K.; Kleßmann, C.; Capone, C.; Stricker, E.; Graus, W.; Hoogwijk, M.; Supersberger, N.; von Winterfeld, U.; Samadi, S. Role and potential of renewable energy and energy efficiency for global energy supply. Report ISSN 1862-4359, German Federal Environmental Agency, 2009.
65. Desing, H.; Brunner, D.; Takacs, F.; Nahrath, S.; Frankenberger, K.; Hischier, R. A Circular Economy within the planetary boundaries: towards a resource-based, systemic approach. *Resources, Conservation and Recycling* **submitted**.